Polymer Journal (2016) 48, 413–419

www.nature.com/pj

ORIGINAL ARTICLE

Platelet-adhesion behavior synchronized with surface rearrangement in a film of poly(methyl methacrylate) terminated with elemental blocks

Hisao Matsuno[1], Ryota Tsukamoto[1], Shinichiro Shimomura[1], Tomoyasu Hirai[1,3], Yukari Oda[1] and Keiji Tanaka[1,2]

Poly(methyl methacrylate) (PMMA) terminated with elemental blocks containing polyhedral oligomeric silsesquioxane (POSS), hereafter referred to as PPMP, was synthesized by living anionic polymerization. Combining modern interfacial-sensitive spectroscopy with traditional contact angle measurements, static and dynamic structures at the surface of PPMP films in water were examined. The surface of the well-annealed PPMP films, where the POSS end groups were preferentially segregated, was flat at the sub-nanometer level. Once the PPMP film was immersed in water, the surface was reorganized, and the rate was much slower for PPMP than for the conventional PMMA. This implies that the POSS units hindered the interfacial dynamics of the polymer segments. Then, platelet-adhesion tests were performed on the PPMP films. The number of platelets adhered to the PPMP film was dependent on the pre-immersion time in phosphate-buffered saline before the platelet seeding, whereas that of the reference PMMA film was unaffected by the pre-immersion time. These results could be explained in terms of the aggregation states of water at the interface.
Polymer Journal (2016) **48,** 413–419; doi:10.1038/pj.2015.118; published online 6 January 2016

INTRODUCTION

Aggregation states and physical properties of polymeric materials have a strong effect on their functions. This is evident even in surface-associated processes, such as wettability, friction and biocompatibility.[1–5] Hence, studies focused on understanding polymer surfaces, especially those investigating actual environment conditions, are promising initiatives for the development of highly surface-functionalized polymeric materials and devices. However, one particular challenge is that because the energy state in the surface and the corresponding bulk regions are not the same,[6–18] the polymer behavior at the surface is difficult to predict based on the analogous characteristics in the bulk.[16–18]

Polymers used in biomedical applications having contact with biogenic substances in water are a notable material of interest. Therefore, the fundamental behavior of these polymers at the water interface should be comprehended and controlled. We studied this issue using a typical glassy polymer, poly(methyl methacrylate) (PMMA), which is used in biomedical tips and artificial intraocular lenses due to its excellent processability, as well as its mechanical and optical properties.[19,20] Once PMMA comes in contact with water, segments in the surface region are partially dissolved in the water phase, and a swollen layer due to water is formed beneath the interface. This leads to faster dynamics of PMMA at the interface compared with that in the bulk.[21–23]

Previously, we successfully constructed polymer surfaces with a nanometer-thick inorganic network structure based on a one-pot sol-gel reaction scheme involving tetraethoxysilane[24,25] and tetraethoxytitanium(IV).[26] Tetraethoxysilane and tetraethoxytitanium(IV) fed into a polymer solution formed an inorganic network before and/or during the film solidification and eventually segregated at the surface of the prepared polymer film. These results in an observed hardness and in antioxidant properties on the polymer surfaces, indicating that the chain dynamics in the surface region must have decelerated due to the presence of inorganic substances.

Here we show that the slower surface reorganization process involving these types of polymers in water. If the dynamics of the water-induced surface reorganization is on the order of 10 h, then the change in the polymer structure and the water aggregation states can be well pursued by interfacial-sensitive spectroscopy. Combining the information that can be obtained from these procedures with the results after a platelet-adhesion assay, a better understanding of the controlling factors for bio-events on the polymer surfaces can be established.

In this study, we focus on polyhedral oligomeric silsesquioxane (POSS),[27–30] rather than tetraethoxysilane, as a regulator of molecular motion at the surface and interfaces of PMMA because the precise control of the acid–base hydrolysis reaction for tetraethoxysilane is particularly challenging under the chosen experimental conditions.

[1]Department of Applied Chemistry, Kyushu University, Fukuoka, Japan and [2]International Institute for Carbon-Neutral Energy Research (WPI-I2CNER), Kyushu University, Fukuoka, Japan
[3]Current address: Institute for Materials Chemistry and Engineering, Kyushu University, Fukuoka 819-0395, Japan.
Correspondence: Dr H Matsuno or Professor K Tanaka, Department of Applied Chemistry, Kyushu University, 744 Motooka, Nishi-ku, Fukuoka 819-0395, Japan.
E-mail: h-matsuno@cstf.kyushu-u.ac.jp or k-tanaka@cstf.kyushu-u.ac.jp
Received 3 October 2015; revised 4 November 2015; accepted 4 November 2015; published online 6 January 2016

POSS is a cubic molecule with an inner inorganic core based on Si–O–Si networks surrounded by various organic functional groups[27–35] and is a promising filler for preparing nano-structured organic–inorganic hybrid materials. Furthermore, POSS has been used as an elementary building block for polymer due to the development of polymerizable POSS-containing chemical compounds.[36–39] In this case, POSS molecules could be well dispersed in the polymer matrix after polymerization, resulting in the elevation of the glass transition temperature (T_g)[40–42] and improvement in the mechanical strength.[43,44] PMMA possessing POSS at both chain ends, hereafter referred to PPMP, was synthesized by living anionic polymerization. The outermost region of the PPMP film was characterized in air and in water. Finally, it is shown that the platelet-adhesion behavior was closely related to the aggregation states of water, or to the fractional amount of disturbed water molecules, at the polymer interface.

EXPERIMENTAL PROCEDURE

Materials

Methyl methacrylate (MMA) and 3-(3,5,7,9,11,13,15-heptaisobutyl-pentacyclo [9.5.1^{3,9}.1^{5,15}1^{7,13}]octasiloxan-1-yl)propyl methacrylate (MAPOSS)[40–45] were used as monomers. PMAPOSS-*b*-PMMA-*b*-PMAPOSS (PPMP), was synthesized by living anionic polymerization in tetrahydrofuran with potassium naphthalenide as an initiator.[46–48] Figure 1 shows a schematic representation of a PPMP chain and its chemical structure. The details of the PPMP synthesis are described in the Supplementary Information. The number-average molecular weight (M_n) and the polydispersity index (M_w/M_n) of PPMP, where M_w is the weight-average molecular weight, were 28.7k and 1.31, respectively, as determined by gel permeation chromatography using PMMA standards. The values of *m* and *n* in Figure 1, or the composition, were determined as 3 and 110, respectively, by ^{1}H-nuclear magnetic resonance spectroscopy with the gel permeation chromatography result. The bulk T_g of PPMP measured using differential scanning calorimetry (Extar6000 DSC6220, Hitachi High-Tech Science Corp., Tokyo, Japan) and defined as a mid-point of the shift in the heat capacity baseline was 397 K. As a reference polymer, monodisperse PMMA with an M_n of 25.0k and a ratio of M_w/M_n of 1.09 was purchased from Polymer Source, Inc. (Montreal, QC, Canada) and was purified by reprecipitation prior to use. The T_g of PMMA was 397 K.

Film preparation

PPMP films were prepared by a conventional spin-coating method from its toluene solution on various solid substrates, such as Si-wafers, borosilicate cover glasses and quartz prisms. The thickness of the PPMP films was ~140 nm. The films were annealed at 433 K in a vacuum oven for 24 h. As a reference, PMMA films were also prepared in the same manner.

Surface characterization

The morphology of the polymer films prepared on the Si-wafers was examined by atomic force microscopy (Agilent Technologies 5500 Scanning Probe Microscope, Agilent Technologies, Inc., Santa Clara, CA, USA) using intermittent contact mode under both air and water environments at room temperature. The cantilever tip used for the measurements was microfabricated from Si, and its spring constant and resonance frequency in air were 2.8 N m^{-1} and 75 kHz, respectively. The tip radius was ~5 nm. The drive frequency used in water was 30 kHz, which was on the low-frequency side of the resonance. To avoid possible deformations of the sample surface during the observation, the ratio of the set point to the free amplitude of the cantilever was maintained at ~0.9 (10% damping of the amplitude of oscillation).

Static contact angle (θ_i) values were examined using a Drop Master 500 (Kyowa Interface Science Co. Ltd., Niiza, Saitama, Japan) at room temperature. As a liquid probe (i), a droplet of ultrapure water (H_2O) purified using a Milli-Q system (Merck Millipore Co., Billerica, MA, USA) and diiodomethane (CH_2I_2) were used for the measurements in air, and a droplet of *n*-heptane (*n*-C_7H_{16}) was used for measurements in water. Furthermore, the contact angles of an air bubble (θ_{air}) for the polymer films were recorded as a function of time immersed in water. The initial θ_{air} value was recorded at 1 min after the immersion of the polymer films, and subsequent immersion times were set to 5 min up to 24 h.

The surface chemical composition of the PPMP film was examined by angular-dependent X-ray photoelectron spectroscopy (PHI 5800 ESCA system, Physical Electronics, Inc., Chanhassen, MN, USA) with a monochromatized Al K_α source. The emission angle (φ_e) was changed from 15° to 90°. The C_{1s} peak was calibrated to a binding energy of 285.0 eV for neutral carbon to correct the charging energy shifts.

Interfacial aggregation states of water as well as polymers were examined by sum-frequency generation (SFG) spectroscopy.[49–51] In this method, a visible beam generated by frequency-doubling the fundamental output pulses from a pico-second Nd:YAG laser (PL2143, EKSPLA) and a tunable infrared (IR) beam generated from an EKSPLA optical parametric generation/amplification and difference frequency generation (OPG/OPA/DFG) system were introduced from the quartz substrate side with incident angles of 50° and 70°, respectively, and were overlapped at a point on the polymer/air or polymer/water interface. SFG spectra were acquired with the polarization combination of *ssp* (SF output, visible input, and IR input), enables the observation of the functional groups oriented normal to the interface. The intensity of the SFG signal was normalized to those of the IR and visible beams.

Platelet adhesion

Platelet-rich plasma extracted from human whole blood was used for the adhesion assay in the same manner as described in the literature.[52,53] Before the tests, the polymer films were immersed in phosphate-buffered saline for a given

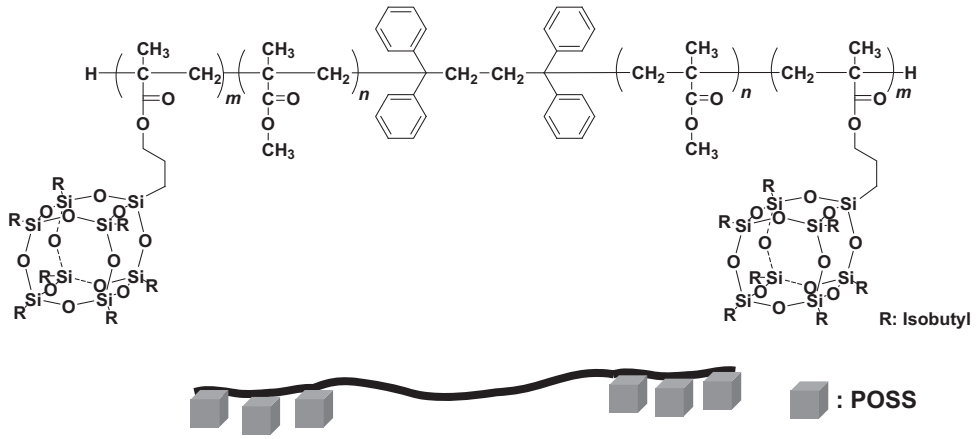

Figure 1 A schematic representation of a POSS-containing block copolymer (PMAPOSS-*b*-PMMA-*b*-PMAPOSS, PPMP) and its chemical structure. The values of *m* and *n* were 3 and 110, respectively. R indicates an isobutyl group covalently bound to Si. Each POSS unit possesses seven isobutyl groups in the outer region. POSS, polyhedral oligomeric silsesquioxane.

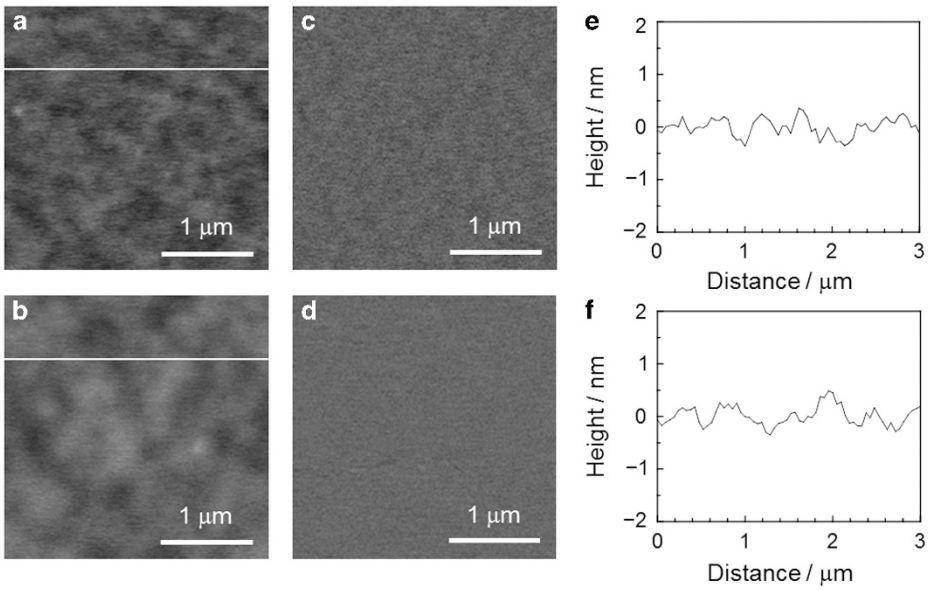

Figure 2 AFM (**a**, **b**) topographic and (**c**, **d**) phase images for (**a**, **c**) PPMP and (**b**, **d**) PMMA films observed in air. (**e**, **f**) Sectional views along each line in **a** and **b**, respectively. AFM, atomic force microscopy; PMMA, poly(methyl methacrylate); PPMP, PMAPOSS-*b*-PMMA-*b*-PMAPOSS.

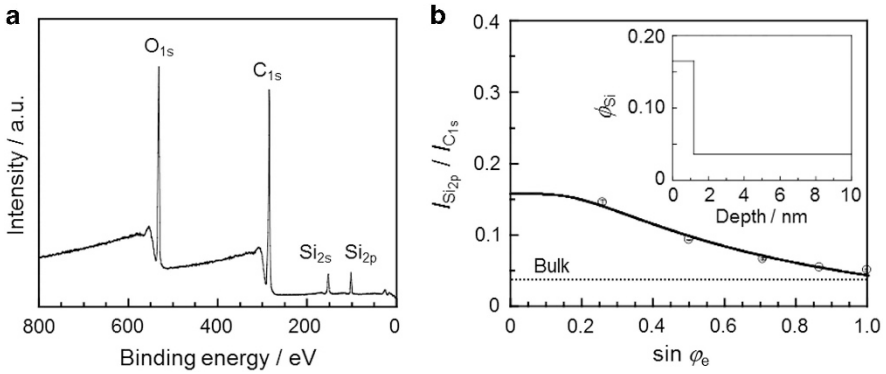

Figure 3 (**a**) XPS survey spectrum at $\varphi_e = 45°$ for a PPMP film annealed at 433 K for 24 h. (**b**) Sin φ_e dependence of the intensity ratio of Si_{2p} and C_{1s} (I_{Si2p}/I_{C1s}). The open circles depict the experimental data, and the solid line is a calculated curve based on the model composition profile of Si (ϕ_{Si}) as a function of depth, as shown in the inset. PMMA, poly(methyl methacrylate); PPMP, PMAPOSS-*b*-PMMA-*b*-PMAPOSS; XPS, X-ray photoelectron spectroscopy.

time. The platelet suspension, with a concentration that was determined by an automated hematology analyzer, was dropped on each film at 310 K (37 °C) for 1 h. After rinsing the polymer films to remove unattached platelets, the adhered platelets were fixed by immersing the films in glutaraldehyde in phosphate-buffered saline. The films were subsequently dried and sputter-coated using a platinum target. The number (N_{PLT}) and the morphology of platelets adhered to the polymer films were examined by scanning electron microscopy (SS-550, Shimadzu, Co., Kyoto, Japan) at an acceleration voltage of 15 kV.

RESULTS AND DISCUSSION

Surface aggregation states

The surface of PPMP films was first characterized. Figure 2 shows topographic images (Figure 2a and b), phase images (Figure 2c and d), and sectional views (Figure 2e and f) for PPMP (Figure 2a, c and e) and PMMA (Figure 2b, d and f) films acquired by atomic force microscopy in air. In all experiments in this study, the data for PMMA are shown as a reference. The root-mean-square surface roughness (R_{RMS}) was 0.24 nm for the PPMP and PMMA films, indicating that these films were sufficiently flat for characterization by the interfacial-sensitive spectroscopy. The phase image for the PPMP film was featureless and was similar to the PMMA film. Hence, it is apparent that POSS units covalently bound to the chain end portions of PMMA were homogeneously dispersed, at least on the outermost surface of the film. This is best suited for our purpose and is in contrast to the results for POSS-containing block copolymers.[44,45] When the length of the POSS units becomes longer, various nanostructures, such as cylinders and lamellae, are formed in the films. This indicates that our design of PPMP with three POSS units at the chain end portions is appropriate for the current purpose.

Static contact angles of water (θ_{H2O}) and diiodomethane (θ_{CH2I2}) for the PPMP and PMMA films were examined, as shown in Supplementary Figure S1a. The data are summarized in Supplementary Table S1. Following Owens' procedure,[54] the surface free energies (γ_S) of the PPMP and PMMA films were determined as 27.7 and 42.6 mJ m^{-2}, respectively. Note that the incorporation of only three POSS units having isobutyl groups on both end portions of PMMA rendered PPMP quite hydrophobic.

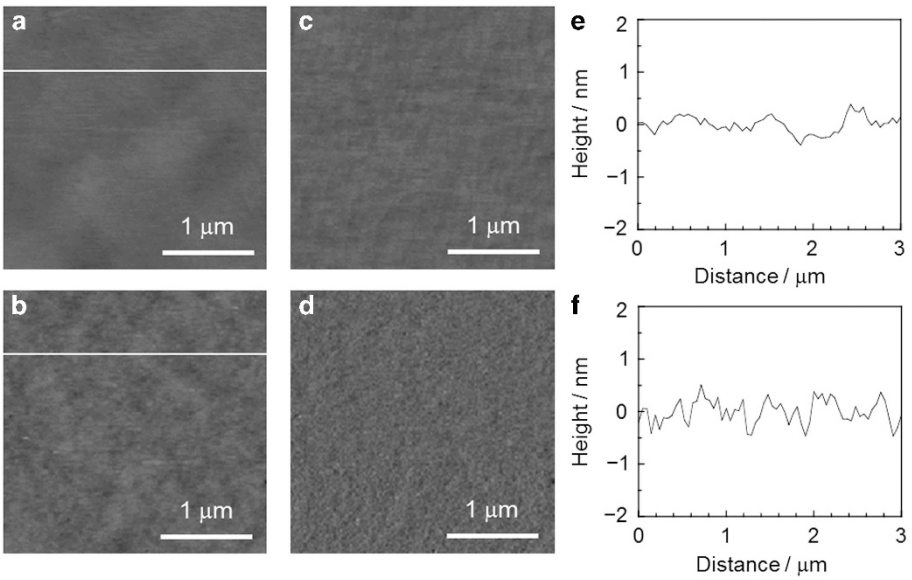

Figure 4 AFM (**a**, **b**) topographic and (**c**, **d**) phase images for the (**a**, **c**) PPMP and (**b**, **d**) PMMA films in water. (**e**, **f**) Sectional views along each line in **a** and **b**, respectively. AFM, atomic force microscopy; PMMA, poly(methyl methacrylate); PPMP, PMAPOSS-*b*-PMMA-*b*-PMAPOSS.

To investigate the hydrophobicity of the PPMP surface, the surface chemical composition was examined by angular-dependent X-ray photoelectron spectroscopy. Figure 3a shows a survey spectrum for the PPMP film obtained at φ_e of 45°. Four peaks at 532, 285, 153 and 102 eV were observed and were attributed to O_{1s}, C_{1s}, Si_{2s}, and Si_{2p}, respectively. Figure 3b shows the sin φ_e dependence of the intensity ratio of Si_{2p} and C_{1s} signals (I_{Si2p}/I_{C1s}). The open symbols denote the experimental data. The I_{Si2p}/I_{C1s} ratio increased with decreasing sin φ_e, indicating that the POSS units containing Si were segregated on the surface region of the film. Although the main panel of Figure 3b provides the information regarding the depth dependence of the composition along the direction normal to the surface from the outermost region, the abscissa is not in the real space. To overcome this problem, a fitting analysis was performed using a simple model; in this case, the film is assumed to be composed of two layers. When a composition profile (ϕ_{Si}) in the real space shown in the inset of Figure 3b is assumed, the best fit to the experimental data is obtained, as drawn by the solid curve in Figure 3b. Thus, it appears most likely that the inorganic layer with a thickness of ~1 nm is formed at the outermost region of the film. This is consistent with the lower γ_S of the PPMP film as previously described. Considering the hydrophobicity of the POSS units, the surface segregation of the POSS units is reasonable.

Water-induced surface reorganization

The aggregation states of PPMP and PMMA at the surface of the films were characterized under an aquatic environment. Figure 4 shows topographic images (Figure 4a and b), phase images (Figure 4c and d) and sectional views (Figure 4e and f) of PPMP (Figure 4a, c and e) and PMMA (Figure 4b, d and f) films immersed in water for 24 h acquired by atomic force microscopy. The R_{RMS} values for the PPMP and PMMA films were 0.22 and 0.28 nm, respectively. These values were essentially the same as those obtained in air, indicating that the surface roughness of both films were nearly unchanged, even in contact with water. In addition, the phase images for both films were again featureless.

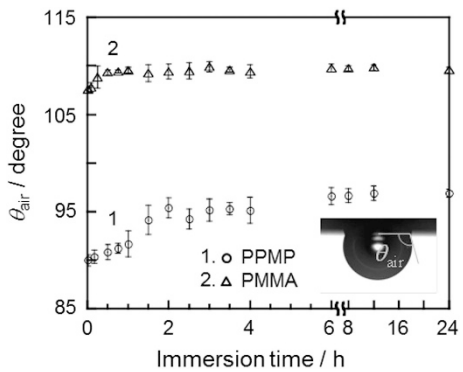

Figure 5 Contact angle of an air bubble (θ_{air}) on the PPMP and PMMA films as a function of time in water. Plots show mean values and standard deviations. PMMA, poly(methyl methacrylate); PPMP, PMAPOSS-*b*-PMMA-*b*-PMAPOSS.

The contact angle of an air bubble (θ_{air}) on the PPMP and PMMA films in water was examined. The measurement is schematically shown in Supplementary Figure S1b, which allows an evaluation of the extent of the hydrophilicity of the surface. Figure 5 shows the immersion-time dependence of θ_{air} on the PPMP and PMMA films. For both films, the θ_{air} value increased with increasing time, indicating that the surfaces of PPMP and PMMA became more hydrophilic in water. However, the time scale of the θ_{air} change was not the same for each film. The initial θ_{air} value for the PPMP film at the immersion time of 1 min was $90.0 \pm 0.6°$. Then, the value continued to increase until ~12 h when it reached a constant of $96.9 \pm 0.7°$. In contrast, the θ_{air} value for the PMMA film rapidly increased from $107.5 \pm 0.3°$ to $109.3 \pm 0.2°$ within a half hour. The interfacial free energies ($\gamma_{S(W)}$) of PPMP and PMMA with water after a 24-h water immersion were estimated as 33.9 and 12.2 mJ m^{-2}, respectively, using an air bubble and a *n*-C_7H_{16} droplet as probes (Supplementary Figure S1b and Supplementary Table S1). Considering that the surface roughness of the PPMP and PMMA films was unchanged in water, it is apparent that the time-dependent change in θ_{air} is caused by a structural reorganization at the water interface.

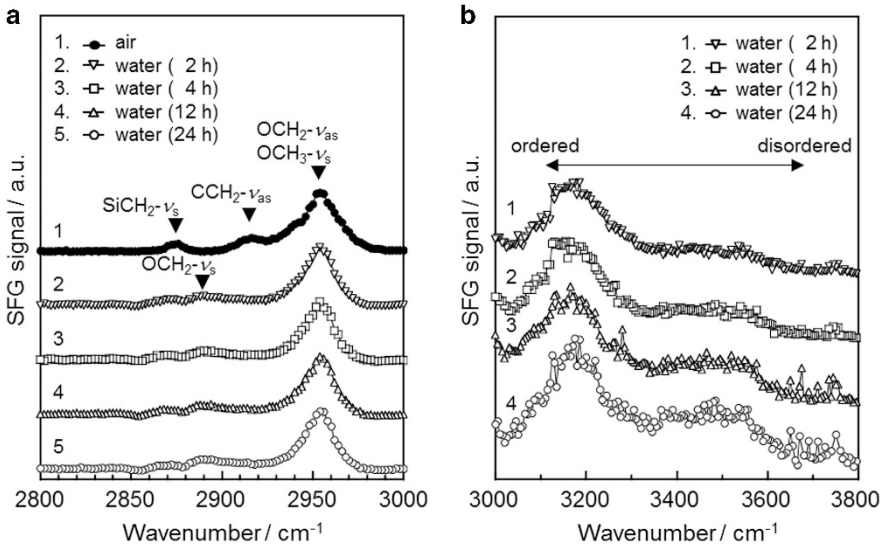

Figure 6 SFG spectra of (**a**) C–H and (**b**) O–H stretching vibration regions with the *ssp* polarization combination for PPMP at the air and water interfaces. For the water interface, spectra were obtained at 2, 4, 12 and 24 h after the immersion. Closed and open symbols denote the experimental signals obtained at air and water interfaces, respectively. PPMP, PMAPOSS-*b*-PMMA-*b*-PMAPOSS; SFG, sum-frequency generation.

Thus, the POSS units hinder the reorganization dynamics in the outermost region of the polymer film in water.

The local conformation of PPMP at the water interface was also examined by SFG.[49–51] Figure 6a shows the SFG spectra for the PPMP films at the air interface and water interface over the C–H stretching region. Because the polarization combination for the sum-frequency, visible and IR beams was *ssp*, the orientation of functional groups along the direction normal to the interface can be discussed. Peaks on the spectra were identified following previous reports about SFG spectra of PMMA[23,55,56] in addition to the Fourier-transform IR spectroscopy measurements for bulk MAPOSS and PPMP samples, as shown in Supplementary Figure S2. For the air interface, one strong peak and two weak peaks were observed. The strong peak at $\sim 2955\ cm^{-1}$ is assignable to the symmetric C–H stretching vibration of ester methyl groups (methoxy groups) (OCH_3-ν_s) at the side chain portion of PMMA[23,55,56] or the asymmetric C–H stretching vibration of ester methylene groups (OCH_2-ν_{as}) at the side chain of PMAPOSS. The peak observed at $\sim 2916\ cm^{-1}$ can be assigned to the asymmetric C–H stretching vibration of methylene groups (CCH_2-ν_{as}) in the main chain part of the polymers. These results indicate that ester methyl groups in the side chains and methylene groups in the main chains are oriented normal to the surface.[23,55,56] In addition, the contribution from the POSS units to the SFG signal was observed. A weak peak at $\sim 2870\ cm^{-1}$ can be attributed to the symmetric C–H stretching vibrations of the CH_2 portion of isobutyl groups ($SiCH_2$-ν_s). This peak assignment is based on the fact that it was not observed for the PMMA film.[23,55,56] This result reveals that the POSS units existed at the outermost surface of the film, which is consistent with the other characterization results.

After the PPMP film was immersed in water for 2 h, the peak pertaining to the methylene groups in the main chain part (CCH_2-ν_{as}) disappeared, indicating that the PPMP main chains were randomized. This conformational change at the water interface was similar to that for PMMA.[23,55,56] In addition, a new peak that can be associated with the symmetric C–H stretching vibrations of the OCH_2 portion (OCH_2-ν_s) at the side chains was observed at $\sim 2890\ cm^{-1}$. Although the immersion time of the film in water became longer, up to 24 h, the spectra did not clearly change. Thus, it appears most likely that the hydrophobic POSS units existed, even at the water interface, and the aggregation states are not changed within the observed time scale of one day.

Figure 6b shows the SFG spectra at different immersion times considering the O–H stretching vibrational region. The SFG signals in this region represent a degree of coordination of water molecules via hydrogen bonding. Signals in the lower and the higher wavenumber regions represent ordered and disordered waters, respectively.[57,58] The local conformation of PPMP chains at the water interface was insensitive to the immersion time, whereas the aggregation states of interfacial water molecules were dependent on the immersion time. At the initial stage (2 h), one broad peak ranging from 3050 to $3350\ cm^{-1}$ was dominant, indicating that relatively ordered water molecules were dominant at the interface. This is in contrast to the PMMA interface where disordered water structures, such as dangling-OH, in addition to ordered ones exist.[23,55,56] As the immersion time increased, the SFG signals derived from the ordered and the relatively disordered water decreased and increased, respectively. In addition, signals at $\sim 3750\ cm^{-1}$ slightly evolved. Areal fractions of the above three peaks were estimated and are summarized in Supplementary Figure S3. Initially, the POSS units with hydrophobic isobutyl groups would enhance the organization of water molecules at the interface due to hydrophobic interactions. Then, the population of more disturbed water molecules increased as the immersion time increased. Interestingly, the time scale of this change is close to the time dependence of θ_{air}, as previously discussed.

Platelet adhesion

The effect of water-induced reorganization of PPMP on its interfacial function was analyzed. Because of its extreme sensitivity to the interfacial properties of polymeric materials, platelets were used as a probe. The polymer films were pre-immersed in an aqueous phosphate-buffered saline solution for a given time before platelet culturing.[52,53] Figure 7a–e show the scanning electron microscopy images of platelets adhered onto the PPMP films with different pre-immersion periods in water. For comparison, the results for the PMMA films are also shown in Figure 7f–j. The number of platelets (N_{PLT}) and its breakdown are classified into three stages based on the

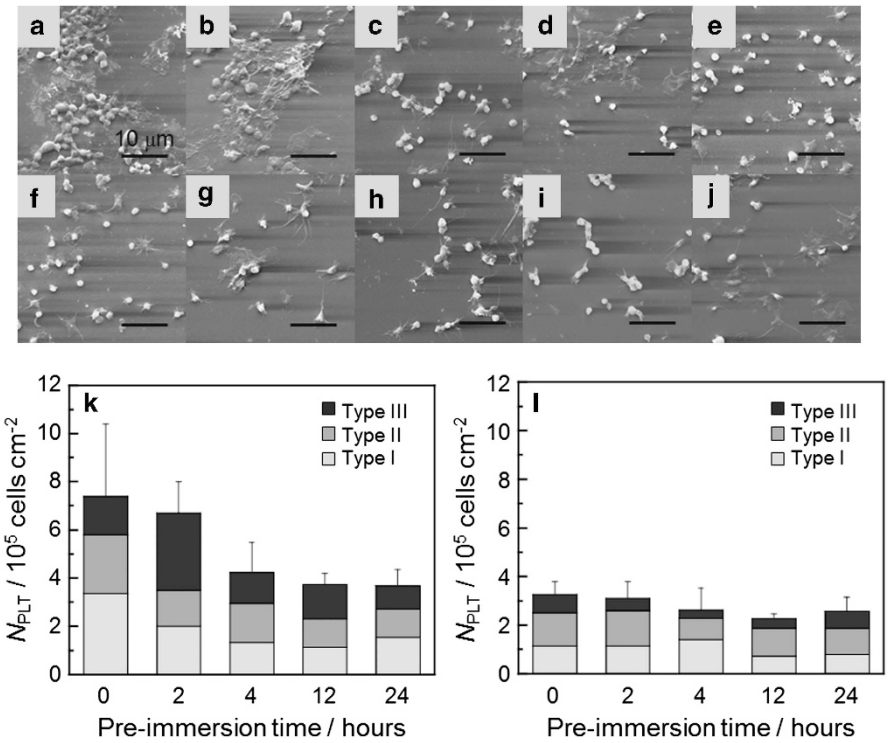

Figure 7 SEM images of platelets adhered for (**a**–**e**) PPMP and (**f**–**j**) PMMA films pre-immersed in an aqueous PBS solution for a given time before platelet seeding. Pre-immersion times were set to (**a**, **f**) 0 h (that is, without pre-immersion), (**b**, **g**) 2 h, (**c**, **h**) 4 h, (**d**, **i**) 12 h and (**e**, **j**) 24 h, respectively. Scale bars correspond to 10 μm. Quantitative data of platelet-adhesion behaviors for (**k**) PPMP and (**l**) PMMA films, respectively. The number of platelets (N_{PLT}) on each sample is shown with the average and standard deviation ($n=5$). The breakdown of N_{PLT} classified into three stages based on the degree of activation of platelet is shown in gray. PBS, phosphate-buffered saline; PMMA, poly(methyl methacrylate); PPMP, PMAPOSS-*b*-PMMA-*b*-PMAPOSS; SEM, scanning electron microscopy.

degree of activation of the platelet: the original spherical shapes (type I), the round shapes with a few protruding pseudopods (type II, partially activated) and the flattened shapes with many pseudopods (type III, strikingly activated). These stages are shown in Figure 7k and l. The N_{PLT} value for the PPMP film without pre-immersion (that is, 0 h) was the largest. In addition, platelets were strikingly activated with many pseudopods (type III) on the film without pre-immersion. The N_{PLT} value for the PPMP films clearly decreased with increasing pre-immersion time up to 12 h, and then, it reached a constant value. The N_{PLT} value for the PMMA film in which the local chain conformation at the water interface was immediately changed was independent of the pre-immersion time. Interestingly, the time scale of the N_{PLT} change observed for PPMP is close to the time dependence of θ_{air}, as shown in Figure 5. Thus, combining Figures 5–7, it appears most likely that the platelet adhesion is closely related to the aggregation states of water or to the fractional amount of disturbed water molecules at the interface.

Considering these results, there are two points for discussion. The θ_{air} on the PPMP film continued to increase up to 12 h. In contrast, the shape of the SFG spectra for the PPMP film in water in the C–H region was insensitive to the immersion time. The time dependence in these two experiments appears to be different, possibly because the aggregation states of water molecules continue to change without involving the reorganization of the polymer at the interface. If that is the case, then our current conclusion that the platelet adhesion is closely related to the aggregation states of water is very appropriate. Another point of discussion is that the local conformation of the polymer at the interface also continued to change. If the conformation is random without any orientations at the interface, then the SFG signals cannot be principally generated. In this case, the platelet adhesion is related to the aggregation states of water and polymer at the interface. Although there is no doubt that the interfacial water structure is one of the controlling factors for the platelet adhesion, further study is required to gain a better understanding of the biocompatibility of polymer materials.

CONCLUSIONS

Static and dynamic surface structures in the films of PMMA terminated with POSS end groups (PPMP) upon the soaking process in water were examined. The POSS units were preferentially segregated at the outermost region of the film. Once the film comes in contact with water, the surface reorganizes, and the rate becomes much slower for PPMP than for PMMA, indicating that the POSS units hindered the interfacial dynamics of the polymer in the film. SFG spectroscopy revealed that the population of more disturbed water molecules increased with increasing immersion time, and the time-scale of this change was close to the time dependence of the surface reorganization. The platelet-adhesion behavior was closely related to the aggregation states of water or to the fractional amount of disturbed water molecules at the interface. We believe that the fundamental knowledge demonstrated in this study is useful for the future development of functionalized polymeric materials.

CONFLICT OF INTEREST

The authors declare no conflict of interest.

ACKNOWLEDGEMENTS

This research was partially supported by the JSPS KAKENHI Grant-in-Aid for Scientific Research on Innovative Areas 'New Polymeric Materials Based on Element-Blocks' (25102535 and 15H00758) program to KT, Grant-in-Aids for

Scientific Research (A) (15H02183) to KT and for Scientific Research (C) (15K05633) to HM. We also appreciate the support from the JST SENTANKEISOKU (13A0004) to KT.

1 Jones, R. A. L. & Richards, R. W. *Polymers at Surfaces and Interfaces* (Cambridge University Press, Cambridge, UK, 1999).
2 Forrest, J. A., Jones, R. A. L. in *Polymer Surfaces, Interfaces and Thin Films* (eds Karim A. & Kumar S.) 251–294 (World Scientific, Singapore, 2000).
3 Kasemo, B. Biological surface science. *Surf. Sci.* **500**, 656–677 (2002).
4 Roach, P., Eglin, D., Rohde, K. & Perry, C. C. Modern biomaterials: a review—bulk properties and implications of surface modifications. *J. Mater. Sci. Mater. Med.* **18**, 1263–1277 (2007).
5 Vasita, R., Shanmugam, I. K. & Katt, D. S. Improved biomaterials for tissue engineering applications: surface modification of polymers. *Curr. Top Med. Chem.* **8**, 341–353 (2008).
6 Reiter, G. Mobility of polymers in films thinner than their unperturbed size. *Europhys. Lett.* **26**, 579–584 (1993).
7 Keddie, J. L., Jones, R. A. L. & Cory, R. A. Size-dependent depression of the glass transition temperature in polymer films. *Europhys. Lett.* **27**, 59–64 (1994).
8 DeMaggio, G. B., Frieze, W. E., Gidley, D. W., Zhu, M., Hristov, H. A. & Yee, A. F. Interface and surface effects on the glass transition in thin polystyrene films. *Phys. Rev. Lett.* **78**, 1524–1527 (1997).
9 Prucker, O., Christian, S., Bock, H., Ruhe, J., Frank, C. W. & Knoll, W. On the glass transition in ultrathin polymer films of different molecular architecture. *Macromol. Chem. Phys.* **199**, 1435–1444 (1998).
10 Fryer, D. S., Nealey, P. F. & de Pablo, J. J. Thermal probe measurements of the glass transition temperature for ultrathin polymer films as a function of thickness. *Macromolecules* **33**, 6439–6447 (2000).
11 See, Y. K., Cha, J., Chang, T. & Ree, M. Glass transition temperature of poly(*tert*-butyl methacrylate) Langmuir–Blodgett film and spin-coated film by X-ray reflectivity and ellipsometry. *Langmuir* **16**, 2351–2355 (2000).
12 Kim, J. H., Jang, J. & Zin, W.-C. Estimation of the thickness dependence of the glass transition temperature in various thin polymer films. *Langmuir* **16**, 4064–4067 (2000).
13 Tsui, O. K. C. & Zhang, H. F. Effects of chain ends and chain entanglement on the glass transition temperature of polymer thin films. *Macromolecules* **34**, 9139–9142 (2001).
14 Kim, J. H., Jang, J. & Zin, W.-C. Thickness dependence of the glass transition temperature in thin polymer films. *Langmuir* **17**, 2703–2710 (2001).
15 Kawana, S. & Jones, R. A. L. Character of the glass transition in thin supported polymer films. *Phys. Rev. E* **63**, 021501 (2001).
16 Fujii, Y., Morita, H., Takahara, A. & Tanaka, K. Mobility gradient of polystyrene in films supported on solid substrates. *Adv. Polym. Sci.* **252**, 1–27 (2013).
17 Tanaka, K., Takahara, A. & Kajiyama, T. Rheological analysis of surface relaxation process of monodisperse polystyrene films. *Macromolecules* **33**, 7588–7593 (2000).
18 Kajiyama, T., Kawaguchi, D., Sakai, A., Satomi, N., Tanaka, K. & Takahara, A. Determination factors on surface glass transition temperatures of polymeric solids. *High Perform. Polym.* **12**, 587–597 (2000).
19 Chen, Y., Zhang, L. & Chen, G. Fabrication, modification, and application of poly (methyl methacrylate) microfluidic chips. *Electrophoresis* **29**, 1801–1814 (2008).
20 Frazer, R. Q., Byron, R. T., Osborne, P. B. & West, K. P. PMMA: an essential material in medicine and dentistry. *J. Long Term Eff. Med. Implants* **15**, 629–639 (2005).
21 Tanaka, K., Fujii, Y., Atarashi, H., Akabori, K., Hino, M. & Nagamura, T. Nonsolvents cause swelling at the interface with poly(methyl methacrylate) films. *Langmuir* **24**, 296–301 (2008).
22 Fujii, Y., Nagamura, T. & Tanaka, K. Relaxation behavior of poly(methyl methacrylate) at a water interface. *J. Phys. Chem. B* **114**, 3457–3460 (2010).
23 Horinouchi, A., Atarashi, H., Fujii, Y. & Tanaka, K. Dynamics of water-induced surface reorganization in poly(methyl methacrylate) films. *Macromolecules* **45**, 4638–4642 (2012).
24 Tsuruta, H., Fujii, Y. & Tanaka, K. One-pot surface modification of rubbery polymer films. *Polym. Chem.* **3**, 319–321 (2012).
25 Tsuruta, H., Ikinaga, Y., Fujii, Y. & Tanaka, K. A simple approach for surface hardening of polystyrene. *Appl. Surf. Sci.* **264**, 589–592 (2013).
26 Matsuno, H., Matsuyama, R., Yamamoto, A. & Tanaka, K. Enhanced cellular affinity for poly(lactic acid) surfaces modified with titanium oxide. *Polymer J.* **47**, 505–512 (2015).
27 Scott, D. W. Thermal rearrangement of branched-chain methylpolysiloxanes. *J. Am. Chem. Soc.* **68**, 356–358 (1946).
28 Baney, R. H., Itoh, M., Sakakibara, A. & Suzuki, T. Silsesquioxanes. *Chem. Rev.* **95**, 1409–1430 (1995).
29 Lichtenhan, J. D. in *Polymeric Materials Encyclopedia: Synthesis, Properties and Applications* (ed. Salamone J. C.) 7768–7778 (CRC Press, Boca Raton, Florida, USA, 1996).
30 Cordes, D. B., Lickiss, P. D. & Rataboul, F. Recent developments in the chemistry of cubic polyhedral oligosilsesquioxanes. *Chem. Rev.* **110**, 2081–2173 (2010).
31 Voronkov, M. G. & Lavrent'yev, V. I. Polyhedral oligosilsesquioxanes and their homo derivatives. *Top. Curr. Chem.* **102**, 199–236 (1982).
32 Murugavel, R., Chandrasekhar, V. & Roesky, H. W. Discrete silanetriols: building blocks for three-dimensional metallasiloxanes. *Acc. Chem. Res.* **29**, 183–189 (1996).
33 Feher, F. J., Newman, D. A. & Walzer, J. F. Silsesquioxanes as models for silica surfaces. *J. Am. Chem. Soc.* **111**, 1741–1748 (1989).
34 Agaskar, P. A. New synthetic route to the hydridospherosiloxanes O_h-$H_8Si_8O_{12}$ and D_{5h}-$H_{10}Si_{10}O_{15}$. *Inorg. Chem.* **30**, 2707–2708 (1991).
35 Sellinger, A. & Laine, R. M. Silsesquioxanes as synthetic platforms. Thermally curable and photocurable inorganic/organic hybrids. *Macromolecules* **29**, 2327–2330 (1996).
36 Haddad, T. S. & Lichtenhan, J. D. Hybrid organic–inorganic thermoplastics: styryl-based polyhedral oligomeric silsesquioxane polymers. *Macromolecules* **29**, 7302–7304 (1996).
37 Pyun, J. & Matyjaszewski, K. The synthesis of hybrid polymers using atom transfer radical polymerization: homopolymers and block copolymers from polyhedral oligomeric silsesquioxane monomers. *Macromolecules* **33**, 217–210 (2000).
38 Mather, P. T., Jeon, H. G., Romo-Uribe, A., Haddad, T. S. & Lichtenhan, J. D. Mechanical relaxation and microstructure of poly(norbornyl-POSS) copolymers. *Macromolecules* **32**, 1194–1203 (1999).
39 Lee, A. & Lichtenhan, J. D. Viscoelastic responses of polyhedral oligosilsesquioxane reinforced epoxy systems. *Macromolecules* **31**, 4970–4974 (1998).
40 Zhang, W. H., Fu, B. X., Seo, Y., Schrag, E., Hsiao, B., Mather, P. T., Yang, N. L., Xu, D. Y., Ade, H., Rafailovich, M. & Sokolov, J. Effect of methyl methacrylate/polyhedral oligomeric silsesquioxane random copolymers in compatibilization of polystyrene and poly(methyl methacrylate) blends. *Macromolecules* **35**, 8029–8038 (2002).
41 Kopesky, E. T., Haddad, T. S., Cohen, R. E. & McKinley, G. H. Thermomechanical properties of poly(methyl methacrylate)s containing tethered and untethered polyhedral oligomeric silsesquioxanes. *Macromolecules* **37**, 8992–9004 (2004).
42 Kopesky, E. T., Haddad, T. S., McKinley, G. H. & Cohen, R. E. Miscibility and viscoelastic properties of acrylic polyhedral oligomeric silsesquioxane–poly(methyl methacrylate) blends. *Polymer* **46**, 4743–4752 (2005).
43 Bizet, S., Galy, J. & Gérard, J.-F. Structure–property relationships in organic–inorganic nanomaterials based on methacryl–POSS and dimethacrylate networks. *Macromolecules* **39**, 2574–2583 (2006).
44 Pyun, J., Matyjaszewski, K., Wu, J., Kim, G.-M., Chun, S. B. & Mather, P. T. ABA triblock copolymers containing polyhedral oligomeric silsesquioxane pendant groups: synthesis and unique properties. *Polymer* **44**, 2739–2750 (2003).
45 Hirai, T., Leolukman, M., Hayakawa, T., Kakimoto, M. & Gopalan, P. Hierarchical nanostructures of organosilicate nanosheets within self-organized block copolymer films. *Macromolecules* **41**, 4558–4560 (2008).
46 Hadjichristidis, N., Pitsikalis, M., Pispas, S. & Iatrou, H. Polymers with complex architecture by living anionic polymerization. *Chem. Rev.* **101**, 3747–3792 (2001).
47 Higashihara, T., Hayashi, M. & Hirao, A. Synthesis of branched polymers by means of living anionic polymerization, 9. Radical coupling reaction of 1,1-diphenylethylene-functionalized polymers with potassium naphthalenide and its application to syntheses of in-chain-functionalized polymers and star-branched polymers. *Macromol. Chem. Phys.* **203**, 166–175 (2002).
48 Ozaki, H., Hirao, A. & Nakahama, S. Polymerization of monomers containing functional silyl groups. 11. Anionic living polymerization of 3-(tri-2-propoxysilyl)propyl methacrylate. *Macromolecules* **25**, 1391–1395 (1992).
49 Shen, Y. R. Surface properties probed by second-harmonic and sum-frequency generation. *Nature* **337**, 519–525 (1989).
50 Hirose, C., Akamatsu, N. & Domen, K. Formulas for the analysis of surface sum-frequency generation spectrum by CH stretching modes of methyl and methylene groups. *J. Chem. Phys.* **96**, 997–1004 (1992).
51 Chen, Z., Shen, Y. R. & Somorjai, G. A. Studies of polymer surfaces by sum frequency generation vibrational spectroscopy. *Ann. Rev. Phys. Chem.* **53**, 437–465 (2002).
52 Hirata, T., Matsuno, H., Kawaguchi, D., Yamada, N. L., Tanaka, M. & Tanaka, K. Effect of interfacial structure on bioinert properties of poly(2-methoxyethyl acrylate)/poly (methyl methacrylate) blend films in water. *Phys. Chem. Chem. Phys.* **17**, 17399–17405 (2015).
53 Hirata, T., Matsuno, H., Kawaguchi, D., Hirai, T., Yamada, N. L., Tanaka, M. & Tanaka, K. Effect of local chain dynamics on a bio-inert interface. *Langmuir* **31**, 3661–3667 (2015).
54 Owens, D. K. & Wendt, R. C. Estimation of the surface free energy of polymers. *J. Appl. Polym. Sci.* **13**, 1741–1747 (1969).
55 Tateishi, Y., Kai, N., Noguchi, H., Uosaki, K., Nagamura, T. & Tanaka, K. Local c of poly(methyl methacrylate) at nitrogen and water interfaces. *Polym. Chem* **1**, 303–311 (2010).
56 Horinouchi, A. & Tanaka, K. An effect of stereoregularity on the structure of poly(methyl methacrylate) at air and water interfaces. *RSC Adv.* **3**, 9446–9452 (2013).
57 Richmond, G. L. Molecular bonding and interactions at aqueous surfaces as probed by vibrational sum frequency spectroscopy. *Chem. Rev.* **102**, 2693–2724 (2002).
58 Oda, Y., Horinouchi, A., Kawaguchi, D., Matsuno, H., Kanaoka, S., Aoshima, S. & Tanaka, K. An effect of side-chain carbonyl groups on the interface of vinyl polymers with water. *Langmuir* **30**, 1215–1219 (2014).

Supplementary Information accompanies the paper on Polymer Journal website (http://www.nature.com/pj)